Analysis of the Plasma Current Profile Driven by Coaxial Helicity Injection in a Tokamak

Cheng Zhang 1), Deng Zhou 1), Sizheng Zhu 1)
1) Institute of Plasma Physics, Chinese Academy of Sciences
P. O. Box 1126, Hefei 230031, P. R. China
E-mail: czhang@mail.ipp.ac.cn

Abstract. The plasma current profile driven by coaxial direct current helicity injection in a low-aspect-ratio toroidal configuration is investigated by applying the principle of minimum energy dissipation rate. It is shown that current profile modes are mainly decided by Lagrange multiplier β. Some critical values of β_c are found. Different current profiles are obtained in different β ranges. Three typical current profiles are presented. The key features agree well with experiment as the first case of $\beta<7$. Large driven plasma current and a typical current profile in a normal tokamak can be obtained in the region of β=7 to 9.65. There exist reversions of both j_φ and B_φ in the central part when β becomes higher than $\beta_c \approx 9.65$. For a selected geometry the values of β_c weakly depend on other parameters. The different β values and corresponding profiles could be achieved by adjusting some parameters. There exist critical values of plasma temperature and bias voltage to induce the transformation of current profile mode. The profile of $\lambda=\mu_0 j_\varphi/B\varphi$ is non-uniform in the plasma and a larger deviation from force free states appears when β becomes higher.

1. Introduction

The idea of helicity injection current drive is based on plasma relaxation processes. To avoid dealing with those complex time-dependent nonlinear relaxation processes, variation principles are employed to predict the features of plasma relaxation. Basically, three different variation principles have been used in plasma physics. The first one is the minimum magnetic energy principle developed by J. B. Taylor [1]. The principle leads to the force-free plasma equilibrium, which has successfully represented reversed-field-pinch (RFP) equilibria. Hameiri and Bhattacharjee [2] proposed the minimum entropy production principle. The principle of minimum rate of energy dissipation was employed by Montgomery and Phillips [3], Wang and Phillips [4], Bevir, Caloutsis and Gimblett [5], and Farengo and Sobehart [6]. To maintain a steady state, helicity must be injected continuously to balance the helicity dissipation. Direct current (dc) helicity injection current drive is one of the attractive methods due to its possibility of high efficiency [7][8]. Experiments on small tokamaks with dc helicity injection have been conducted [8-11]. The toroidal current obtained on the Helicity Injected Tokamak (HIT) [8][11] reached up to 200 kA. The EFIT reconstructed equilibria [12] [13] show a considerable closed flux on HIT. On the theoretical side, Farengo and Sobehart [6] gave a prediction of driven current and magnetic field profile by employing the minimum dissipation principle in an infinite-length straight plasma. An analysis of the relaxed state for coaxial helicity injection current drive in toroidal plasmas and a good agreement with the experiments are given by Zhang et al. [14]. In this paper, different plasma current profiles driven by coaxial direct current helicity injection in a low-aspect-ratio toroidal configuration are investigated by applying analytical and numerical methods. The analyses indicate that current profile modes are mainly decided by Lagrange multiplier β. Three different typical current profiles are obtained in different ranges of β. Each profile can be realized by adjusting some controllable parameters.

2. Physical Model

A low-aspect-ratio tokamak with R=0.3m, a=0.2m as shown in Fig. 1 is used. The boundary shape is assumed to be a square and the vertical height of the vessel is h=0.68m. This is a simplified version of the HIT device. A, B, C and D form the container, A and C are electrodes, B and D are insulators, C consists of C1, C2 and C3. A bias voltage is applied between A and C, helicity is injected continuously to balance the helicity dissipation $V_{inj}\phi_B = \int_V \eta \vec{j}\cdot\vec{B}d\tau$, where ϕ_B is the poloidal flux through boundary A, η is resistivity, V_{inj} is the bias voltage. With the Gauss theorem and helicity balance as two constraints, the variation function is $W = \int_V \eta j^2 d\tau - \beta\left[\int_V \eta\vec{j}\cdot\vec{B}d\tau + \oint\varphi\vec{B}\cdot d\vec{\sigma}\right] - \int_V \gamma\nabla\cdot\vec{B}d\tau$ (1)

With a variation $\delta W = 0$, we get the Euler-Lagrange equations in cylindrical coordinate

$$\frac{1}{r}\frac{\partial}{\partial r}\left(r\frac{\partial j_\varphi}{\partial r}\right) + \frac{\partial^2 j_\varphi}{\partial z^2} - \frac{j_\varphi}{r^2} + \beta^2 j_\varphi = 0 \qquad (2a)$$

$$\frac{1}{r}\frac{\partial}{\partial r}\left(r\frac{\partial B_\varphi}{\partial r}\right) + \frac{\partial^2 B_\varphi}{\partial z^2} - \frac{B_\varphi}{r^2} + \beta j_\varphi = 0 \qquad (2b)$$

$$\frac{\partial}{\partial r}\left(\frac{1}{r}\frac{\partial\psi}{\partial r}\right) + \frac{1}{r}\frac{\partial^2\psi}{\partial z^2} + j_\varphi = 0 \qquad (2c)$$

Where $\vec{B} = (1/r)(\nabla\psi\times\vec{e}_\varphi) + B_\varphi\vec{e}_\varphi$, ψ is poloidal magnetic flux, β is Lagrange multiplier.

Electric potential is supposed to satisfy the Laplace equation. The normal current density is $j_n = E_n/\eta_{ed}$, η_{cd} is the effective resistivity in the boundary layer, j_n=0 on isolator layers B and D. On boundaries A, C2: $\partial B_\varphi/\partial z = -j_r$, on boundaries B, D, C1,C3: $\partial(rB_\varphi)/\partial r = rj_z$. A natural boundary condition $j_{\varphi b} = \beta B_{\varphi b}/2$ from variation is given.

3. Analytical and Numerical Results

3.1 Analytical j_φ Solution of Euler-Lagrange Equations

Taking j_ϕ into two parts, we have the j_φ solution of Euler-Lagrange equations as the sum of two convergent infinite series

$$j_\varphi = \Psi_1(r,z) + \Psi_2(r,z) \qquad (3).$$

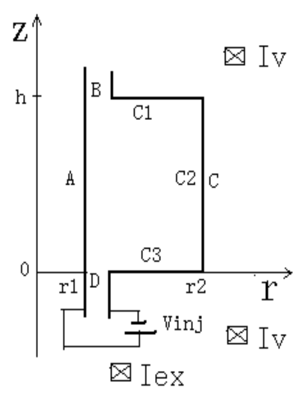

Fig. 1.Configuration of a low-aspect-ratio tokamak

For $k_n^1 < \beta < k_{n+1}^1$

$$\Psi_2(r,z) = \sum_{m=1}^{n} \frac{J_1(k_m^1 r)}{\sin(u_m h)}\left[Q_m \sin(u_m z) + P_m \sin(u_m(h-z))\right] + \sum_{m=n}^{\infty} \frac{J_1(k_m^1 r)}{\sinh(u_m h)}\left[Q_m \sinh(u_m z) + P_m \sinh(u_m(h-z))\right] \tag{4}$$

with $u_m{}^2 = \beta^2 - (k_m^1)^2$ for $1 \le m \le n$ and $u_m{}^2 = (k_m^1)^2 - \beta^2$ for $m \ge n+1$.

$R(r) = J_1(k_m^1 r)$ is the first kind Bessel function of order 1, $k_m^1 = x_m^1 / r_0$, and x_m^1 is the mth zero point of the Bessel function.

Let $v_n = n\pi / h$ with n a positive integer number. For $v_m \le \beta < v_{m+1}$, the solution is

$$\Psi_1(r,z) = \sum_{n=1}^{m} \left[c_n J_1(k_n r) + d_n Y_1(k_n r)\right]\sin(v_n z) + \sum_{n=m+1}^{\infty} \left[c_n I_1(k_n r) + d_n K_1(k_n r)\right]\sin(v_n z) \tag{5}$$

P_m, Q_m, c_n and d_n are obtained by applying the boundary conditions.

From the boundary conditions $j_{\varphi b}=(\beta/2)B_{\varphi b}$ and the solving process, we find that for a selected geometry the solution of j_φ can be easily expressed as $(\beta/2)F(\beta, V_{inj}/\eta_{ed}, B_V, r, z)$. Then the toroidal magnetic flux density can be written as the sum of two parts: $B_\varphi = F(\beta, V_{inj}/\eta_{ed}, B_V, r, z)/2 + F(0, V_{inj}/\eta_{ed}, B_V, r, z)/2$, where the first term satisfies Eq. (2b) and a boundary value $B_{\varphi b}/2$, while the latter part satisfies the corresponding homogeneous equation and a boundary value $B_{\varphi b}/2$.

3.2 Lagrange Multiplier β and Three Typical Current Profiles

The scan of parameters for the solution shows that current profile modes are mainly decided by Lagrange multiplier β. Some critical values of β_c are found, which weakly depend on V_{inj}/η_{ed} and B_v. The same mode of plasma current profile is obtained in one β range and quite different current profiles are obtained in different β ranges. Our results show that three typical current profiles exist in different ranges of β values. The equatorial plane current

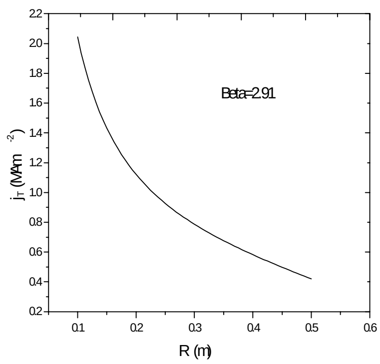

Fig. 2. Typical mid-plane j_φ profile for low beta values.

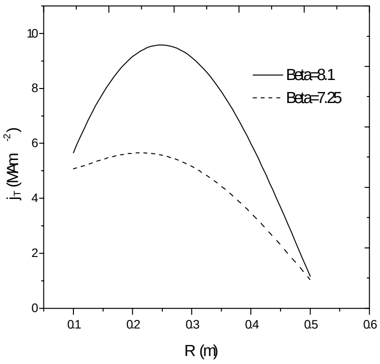

Fig. 3. Typical mid-plane j_φ profile for β=7.1- 9.65

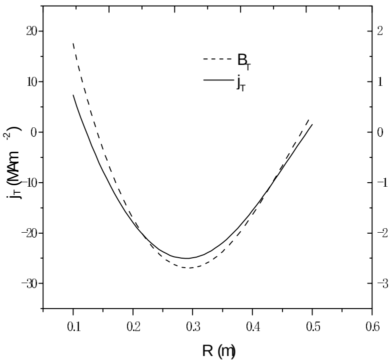

Fig. 4 The mid-plane profiles of j_φ (solid line) and B_φ (dashed line) for β=10.5.

profiles for a set of parameters V_{inj}=700 V, $\eta_{ed}=2.1\times10^{-2}$ Ωm and B_V=0.5 T are illustrated in Figs 2-4. The first kind distribution for $\beta<7.1$ as shown in Fig. 2 is a typical state in the present experiments on HIT. Numerical simulation indicates that the key features such as total toroidal driven current, current in closed field, current density profile, and magnetic configuration agree well with experiments on HIT and in this case $\beta=2.91$. The second kind for $7.1 < \beta < 9.65$ in Fig. 3 shows a typical form for general tokamaks. Much larger driven currents than the first case are expected. Total driven currents are 998.4kA and 1513.1kA for $\beta=7.3$ and $\beta=8.0$ respectively. The first kind transfers continuously to the second kind when β increases up to a value around 7.1, but the distribution changes violently, like a phase transition, when the β value changes from below a critical β_c~9.65 to above it. Both j_φ and B_φ in the central part are reversed when β is higher than $\beta_c\approx9.65$. Their reversion points are quite close to each other when β is near β_c. We have not considered those β values larger than 16.0.

3.3 Dependence of β value on experimental parameters

For a selected geometry, the values of β_c are weakly dependent on experimental parameters. However different β and the corresponding profiles, as well as driven current values, can be achieved by adjusting parameters like V_{inj}, η, η_{ed}, B_V, and currents of bias coils. Two examples from numerical simulation are presented. The first has been shown in Figs 2-4, in which the same parameters are taken except for $\eta=3.8\times10^{-6}$Ωm in Fig. 2, 9.0×10^{-7}Ωm, 4.5×10^{-7}Ωm in Fig. 3 and 2.25×10^{-7}Ωm in Fig. 4. Corresponding electron temperature values are 55.22eV, 144.27eV, 229.01eV and 363.54eV for Z_{eff}=2. It is shown in Fig. 5 that plasma temperature is higher in a higher β state, especially a reversed-field state. The second example is, as the result of adjusting V_{inj} with other parameters kept the same ($\eta=2.18\times10^{-6}$Ωm and $\eta_{ed}=1.0\times10^{-2}$Ωm) shown in Fig. 6.The relaxed state with high β will be obtained by applying a high V_{inj}. From Fig. 5 and Fig. 6 we can see that there exist critical temperature and V_{inj} values to induce the transformation of current profile mode.

3.4 Deviation away from force free states

The profile of $\lambda=\mu_0 j_\varphi/B_\varphi$ is non-uniform in the plasma and a larger deviation from force free states appears when β becomes higher. In different β ranges the plasma relaxes to different

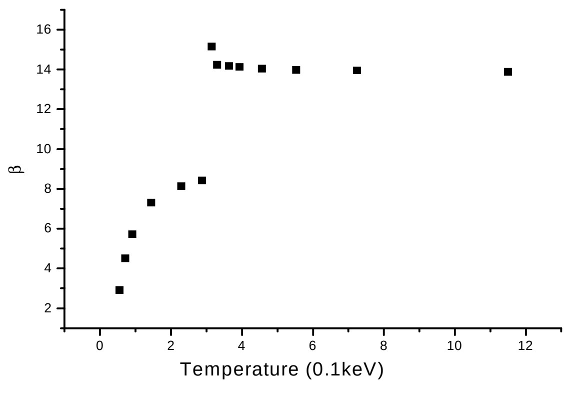

Fig. 5. Dependence of β on Te, showing transfer to reversed-field state at critical Te.

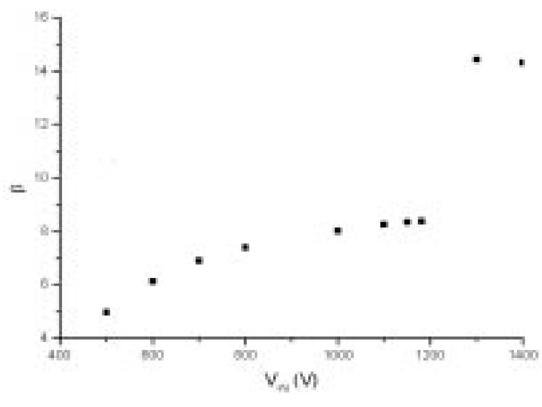

Fig. 6. Dependence of β on Vinj, showing transfer to reversed-field state at critical Vinj

states. The second term $F(0, V_{inj}/\eta_{ed}, B_V, r, z)/2$ of B_φ is always a decreasing function of radius r, similar to that shown in Fig. 2, while the first term is in proportion to j_φ. So for low β values, the plasma drifts away from the force free state weakly, but deviates quite a lot from it when the β value increases.

4. **Summary**

An analysis from the minimum energy dissipation principle for a plasma relaxed state driven by helicity injection is presented. Different current profile modes are mainly decided by Lagrange multiplier β. Some critical values of β_c are found. Three typical plasma current profiles are presented. Both j_φ and B_φ in the central part are reversed when β is higher than $\beta_c \approx 9.65$. For a selected geometry the values of β_c are weakly dependent on experimental parameters. The different β values and corresponding profiles could be achieved by adjusting some parameters. The profile of $\lambda = \mu_0 j_\varphi / B\varphi$ is non-uniform in the plasma and a larger deviation from force free states appears when β becomes higher.

This work is supported by the National Science Foundation of China (No. 19785004).

[1] TAYLOR, J. B., "Relaxation of toroidal plasma and generation of reverse magnetic fields", Phys. Rev. Lett. **33** (1974) 1139.
[2] HAMEIRI, E., et al., "Entropy production and plasma relaxation", Phys. Rev. A **35** (1987) 768.
[3] MONTGOMERY, D., et al., "Minimum dissipation rates in magnetohydrodynamics", Phys. Rev. A **38** (1988) 2953.
[4] WANG, C. Y., et al., "Optimum theory for the energy dissipation in a turbulent pinch", Phys. Fluids B **3** (1991) 3462.
[5] BEVIR, M. K., et al., "A note on minimum dissipation plasma states", Plasma Phys. Controlled Fusion **34** (1993) 133.
[6] FARENGO, R., et al., "Minimum ohmic dissipation and DC helicity injection in tokamak-like plasmas", Plasma Phys. Controlled Fusion **36** (1994) 1691.
[7] JENSEN, T. H., et al., "Current drive and helicity injection", Phys. Fluids **27** (1984) 2881.
[8] JARBOE, T. R., "Formation and steady-state sustainment of a tokamak by coaxial helicity injection", Fusion Technol. **15** (1989) 7.
[9] ONO, M., et al., "Steady-state tokamak discharge via dc helicity injection", Phys. Rev. Lett. **59** (1987) 2165.
[10] DARROW, D. S., et al., "Properties of dc helicity injected tokamak plasmas", Phys. Fluids B **2** (1990) 1415.
[11] NELSON, B. A., et al., "Formation and sustainment of a 150kA tokamak by coaxial helicity injection", Phys. Rev. Lett. **72** (1994) 3666.
[12] LAO, L. L., et al., "Reconstruction of current profile parameters and plasma shapes in tokamaks", Nuclear Fusion **25**, (1985) 1611.
[13] ZHANG, Cheng, et al., "Equilibrium studies on the helicity injected tokamak", Bull. Am. Phys. Soc. **38** (1993) 2010.
[14] ZHANG, Cheng, et al., "Relaxed state for the coaxial helicity injection current drive in toroidal plasmas", Phys. Plasmas **5** (1997) 178.